

94-1

CRREL REPORT

AD-A278 154



2  
DTIC  
ELECTE  
APR 13 1994  
S G D



## Growth Condition of an Ice Layer in Frozen Soils Under Applied Loads

### 2: Analysis

Yoshisuke Nakano and Kazuo Takeda

January 1994



94 4 13 002

**Abstract**

The results of an experimental study on the steady growth condition of a segregated ice layer under various applied pressures were presented in Part 1. Using the data obtained, we evaluate the accuracy of the model  $M_1$ , and the predicted steady growth condition is found to be in good agreement with the condition found empirically. The concept of segregation potential introduced by Konrad and Morgenstern in the early 1980s is examined based on  $M_1$ .  $M_1$  is found to be consistent with the empirical data that were used to support their segregation potential theory.

*Cover: Apparatus for testing ice growth in soils under applied loads. (Photo by K. Takeda.)*

For conversion of SI metric units to U.S./British customary units of measurement consult *Standard Practice for Use of the International System of Units (SI)*, ASTM Standard E380-89a, published by the American Society for Testing and Materials, 1916 Race St., Philadelphia, Pa. 19103.



**US Army Corps  
of Engineers**

**Cold Regions Research &  
Engineering Laboratory**

## **Growth Condition of an Ice Layer in Frozen Soils Under Applied Loads**

### **2: Analysis**

Yoshisuke Nakano and Kazuo Takeda

January 1994

Accession For	
NTIS	CRA&I
DTIC	TAB
Unannounced	
Justification _____	
By _____	
Distribution / _____	
Availability Codes	
Dist	Avail and / or Special
A-1	

Prepared for  
OFFICE OF THE CHIEF OF ENGINEERS

**DTIC QUALITY INSPECTED 3**

Approved for public release; distribution is unlimited.

## PREFACE

This report was prepared by Dr. Yoshisuke Nakano, Chemical Engineer, of the Applied Research Branch, Experimental Engineering Division, U. S. Army Cold Regions Research and Engineering Laboratory, and by Dr. Kazuo Takeda of the Technical Research Institute, Konoike Construction Co., Ltd., Konohana, Osaka, Japan. Funding for Dr. Nakano's research was provided by DA Project 4A161102AT24, *Research in Snow, Ice and Frozen Ground*, Task SC, Work Unit F01, *Physical Processes in Frozen Soil*. Dr. Takeda's experimental work was funded by Konoike Construction Company.

The authors thank Dr. Virgil Lunardini and Dr. Y.C. Yen of CRREL for their technical review of this report.

The contents of this report are not to be used for advertising or promotional purposes. Citation of brand names does not constitute an official endorsement or approval of the use of such commercial products.

## CONTENTS

	Page
Preface .....	ii
Nomenclature .....	iv
Introduction .....	1
Properties of $M_1$ .....	4
Model $M_1$ and segregation potential .....	8
Results of data analysis .....	11
1. Steady growth condition .....	11
2. Dependence of $y^*$ on $T_1^*$ .....	13
3. Dependence of $T_1^*$ on $f_{10}^*$ .....	15
Discussion and conclusions .....	17
Literature cited .....	18
Abstract .....	19

## ILLUSTRATIONS

### Figure

1. A steadily growing ice layer in a freezing soil .....	1
2. An essential frozen fringe $R_{11}$ .....	2
3. Temperature gradients $\alpha_1$ and $\alpha_0$ .....	3
4. Trajectories $\alpha(t)$ that approximately describe the condition of freezing at the formation of the final ice lens .....	9
5. Values of $SP_0$ vs. the values of the average temperature gradient .....	10
6. Values of $y^*$ vs. $\alpha_0$ under various applied pressures $\sigma$ .....	12
7. Average values $y_a^*$ vs. $\sigma$ .....	12
8. Values of $y^*$ vs. the temperature $-T_1^*$ under various applied pressures $\sigma$ .....	14
9. Values of $-T_1^*$ vs. the mass flux of water $f_{10}^*$ under various applied pressures $\sigma$ .....	15
10. Values of $-T_1^*$ vs. the flux $f_{10}^*$ under various applied pressures $\sigma$ .....	17

## TABLES

### Table

1. Calculated values $\bar{y}^*$ and the average measured values $\bar{y}^*$ under various applied pressures $\sigma$ .....	12
2. Summary of data analysis with $\sigma = 48.7$ kPa .....	13

## NOMENCLATURE

*a* function defined by eq 11a  
*a<sub>e</sub>* function defined by eq 27f  
*a<sub>i</sub>* constant where  $i = 0, 1, \dots 3$   
 $\hat{a}_i$  function defined by eq 25d and 25e, where  $i = 0, 1$   
*A* constant  
*b* function defined by eq 11b  
*b<sub>i</sub>* constant where  $i = 1, 2$ .  
*B<sub>i</sub>*  $i$ th constituent of the mixture. Subscripts  $i = 1, 2$ , and 3 are used to denote unfrozen water, ice and soil minerals, respectively  
*c<sub>i</sub>* heat capacity of the  $i$ th constituent  
*d* unit of time (day)  
*d<sub>i</sub>* density of the  $i$ th constituent  
*e* void ratio  
*f<sub>i</sub>* mass flux of the  $i$ th constituent relative to that of soil minerals where  $i = 1, 2$   
*f<sub>10</sub>* mass flux of water in the unfrozen part of the soil  
*I* function defined by eq 16b  
*k* thermal conductivity of a frozen fringe defined by eq 9a  
*k<sub>0</sub>* thermal conductivity of the unfrozen part of the soil  
*k<sub>1</sub>* thermal conductivity of an ice layer  
*k<sub>01</sub>* limiting value of *k* defined by eq 9c  
*K<sub>0</sub>* hydraulic conductivity in the unfrozen part of the soil  
*K<sub>i</sub>* empirical function defined by eq 4a where  $i = 1, 2$   
*K<sub>11</sub>* limiting value of *K<sub>i</sub>* as  $x$  approaches  $n_1$  while  $x$  is in  $R_1$ ,  $i = 1, 2$   
*K<sub>10</sub>* limiting value of *K<sub>i</sub>* as  $x$  approaches  $n_0$  while  $x$  is in  $R_1$ ,  $i = 1, 2$   
*L* latent heat of fusion of water,  $334 \text{ J g}^{-1}$   
*m* location of the free end of the column  
*M<sub>i</sub>* name of a model where  $i = 1, 2, 3$   
*n* boundary in  $R_0$   
*n<sub>i</sub>* boundary with  $i = 0, 1$  where  $n_0$  denotes the boundary where  $T = 0^\circ\text{C}$  and  $n_1$  the interface between an ice layer and a frozen fringe  
*n<sub>10</sub>* boundary between  $R_{10}$  and  $R_{11}$   
*p<sub>0</sub>* gravity term,  $0.098 \text{ [kPa/cm]}$   
*P<sub>i</sub>* pressure of the  $i$ th constituent where  $i = 1, 2$   
*P<sub>10</sub>* value of *P<sub>1</sub>* at  $n_0$   
*P<sub>1n</sub>* value of *P<sub>1</sub>* at  $n$   
*P<sub>21</sub>* value of *P<sub>2</sub>* at  $n_1$

$r$  rate of heave  
 $R_0$  unfrozen part of the soil  
 $R_1$  frozen fringe  
 $R_{10}$  part of the soil bounded by  $n_0$  and  $n_{10}$   
 $R_{11}$  essential frozen fringe  
 $R_2$  ice layer  
 $R_m$  region in the diagram of temperature gradients where an ice layer melts  
 $R_s$  region in the diagram of temperature gradients where the steady growth of an ice layer occurs  
 $R_s^*$  boundary between  $R_s$  and  $R_u$   
 $R_s^{**}$  boundary between  $R_m$  and  $R_s$   
 $R_u$  region in the diagram of temperature gradients where the steady growth of an ice layer does not occur  
 $S$  property of a given soil  
 $SP_0$  segregation potential defined by eq 2a  
 $t$  time  
 $T$  temperature  
 $T_1$  temperature at  $n_1$   
 $T_{10}$  defined by eq 41  
 $T_{11}$  calculated value of  $T_1$  from the measured temperature profile in  $R_2$   
 $\hat{T}_1^*$  empirically determined value of  $T_1^*$   
 $T_1^{**}$  temperature at  $n_1$  when eq 1 holds true  
 $\hat{T}_0$  constant  
 $(T')_a$  average temperature gradient in  $R_1$   
 $\Delta T$  defined by eq 3c  
 $x$  spatial coordinate  
 $y$  variable defined by eq 17c  
 $\bar{y}$  variable defined by eq 38b  
 $y_a$  variable defined by eq 3a  
 $\alpha(t)$  trajectory  $[\alpha_1(t), \alpha_0(t)]$  in the diagram of temperature gradients  
 $\alpha_0$  absolute value of the temperature gradient at  $n_0$   
 $\alpha_1$  absolute value of the limiting temperature gradient as  $x$  approaches  $n_1$  while  $x$  is in  $R_2$ , defined by eq 6  
 $\alpha_f$  absolute value of the temperature gradient near  $n_1$  in  $R_2$   
 $\alpha_u$  absolute value of the temperature gradient near  $n_0$  in  $R_0$   
 $\beta_0$  defined by eq 11c  
 $\gamma$  constant,  $1.12 \text{ MPa } ^\circ\text{C}^{-1}$   
 $\gamma_1$  defined by eq 24b  
 $\delta$  thickness of a frozen fringe  
 $\delta^{**}$  defined by eq 27b  
 $\delta_e$  thickness of an essential frozen fringe defined by eq 27a  
 $\delta_0$  defined by eq 13c

$\eta$  defined by eq 9b

$\rho$  composition of the soil

$\rho_i$  bulk density of the  $i$ th constituent

$\sigma$  effective pressure defined by eq 1 and 16c

$\phi_0$  empirical function of  $T$  defined by eq 14a

$\phi_{01}$  value of  $\phi_0$  at  $T = T_1$

$\phi_1$  empirical function of  $T$  defined by eq 14b

$\phi_{11}$  value of  $\phi_1$  at  $T = T_1$

$\varphi_0$  variable defined by eq 21b

$\varphi_1$  variable defined by eq 25f

$\omega_i$  dimensionless quantity defined by eq.18a through 18d where  $i = 0, 1, \dots, 3$

$i$  subscript denotes the  $i$ th constituent of the mixture consisting of unfrozen water ( $i = 1$ ), ice ( $i = 2$ ) and soil minerals ( $i = 3$ )

\* superscript used to indicate the value of any variable evaluated when a point  $(\alpha_1, \alpha_0)$  in the diagram of temperature gradients is on  $R_s^*$

\*\* superscript used to indicate the value of any variable evaluated when a point  $(\alpha_1, \alpha_0)$  in the diagram of temperature gradients is on  $R_s^{**}$

## Growth Condition of an Ice Layer in Freezing Soils Under Applied Loads

### 2. Analysis

YOSHISUKE NAKANO AND KAZUO TAKEDA

#### INTRODUCTION

In this report we will consider the one-directional steady growth of an ice layer. Let the freezing process advance from the top down and the coordinate  $x$  be positive upwards, with its origin fixed at some point in the unfrozen part of the soil. A freezing soil in this problem may be considered to consist of three parts: the unfrozen part  $R_0$ , the frozen fringe  $R_1$  and the ice layer  $R_2$ , as shown in Figure 1. The physical properties of parts  $R_0$  and  $R_2$  are well understood but our knowledge on the physical properties and the dynamic behavior of part  $R_1$  does not appear sufficient for engineering applications.

It has been shown empirically (Radd and Oertle 1973, Takashi et al. 1981) that there is a unique temperature  $T_1^{**}$  at  $n_1$  for a given pressure of ice  $P_{21}$  at  $n_1$  and a given pressure of water  $P_1$  in  $R_0$  when an existing ice layer neither grows nor melts and the mass flux of water  $f_1$  in  $R_1$  vanishes. This temperature  $T_1^{**}$  at the phase equilibrium of water is given as

$$\sigma = P_{21} - P_1 = -\gamma T_1^{**}, \quad \text{if} \quad f_1 = 0 \quad (1)$$

where  $\gamma$  is a constant with the value of  $1.12 \text{ MPa } ^\circ\text{C}^{-1}$ , and  $\sigma$  and  $P_{21}$  are often referred to as the effective pressure and the overburden pressure, respectively. Equation 1 is often called the generalized Clausius-Clapeyron equation, which is attributed to Edlefsen and Anderson (1943).

Konrad and Morgenstern (1980, 1981, 1982) empirically found that the rate of water intake  $f_{10}$  at the formation of the final ice lens is proportional to the average temperature gradient  $(T') in the frozen fringe. This may be written as$

$$f_{10} = -SP_0(T')_a \quad (2a)$$

where a prime denotes differentiation with respect to  $x$ . The positive proportionality factor  $SP_0$  is termed the segregation potential, which is a property of a given soil. Konrad and Morgenstern also found empirically that  $SP_0$  is a decreasing function of both the applied pressure  $\sigma$  and the suction of water ( $-P_{10}$ ) at  $n_0$ . We will write this dependence as

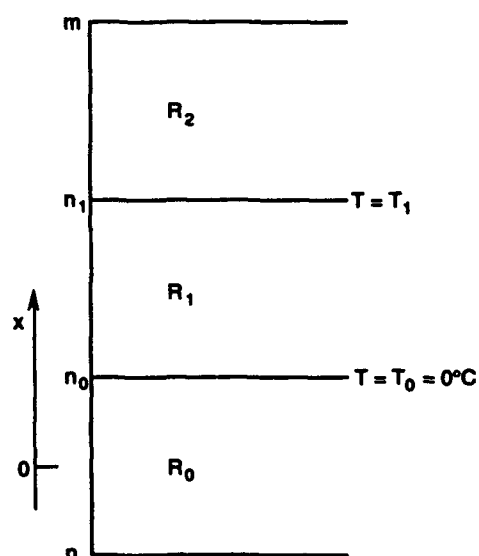


Figure 1. Schematic of a steadily growing ice layer in a freezing soil.

erally depend on the temperature  $T$  and the composition of the soil. We will describe such functional dependence of  $K_i$  ( $i = 1, 2$ ) as

$$K_1 = K_1(T, \rho) \quad (4d)$$

$$K_2 = K_2(T, \rho) \quad (4e)$$

where  $\rho$  symbolically denotes the composition of the soil that is uniquely determined by the bulk densities of unfrozen water  $\rho_1$ , ice  $\rho_2$  and soil minerals  $\rho_3$ .

Nakano (1990) obtained the exact mathematical solution to the problem of a steadily growing ice layer based on the model  $M_1$ . Analyzing the behavior of this solution, we showed that  $M_1$  is consistent with eq 1 (Nakano 1990) and eq 3b (Nakano and Takeda 1991). We also showed (Nakano and Takeda 1991) that  $M_1$  can accurately describe the steady growth condition of an ice layer under negligible applied pressures.

The steady growth condition of an ice layer with or without applied pressure is the region  $R_s$  bounded by a curve  $R_s^*$  and a straight line  $R_s^{**}$  in the diagram of temperature gradients as shown in Figure 3. The region  $R_s$  is defined as

$$(k_1/k_0)\alpha_1 > \alpha_0 > k_1(k_0 + LbK_{21}^*)^{-1}\alpha_1 \quad (5)$$

where  $k_1$  and  $k_0$  are the thermal conductivities of  $R_2$  and  $R_0$ , respectively,  $\alpha_0$  is the absolute value of the temperature gradient at  $n_0$  and  $\alpha_1$  is the limiting value of the temperature gradient at  $n_1$  in  $R_2$  defined as

$$\alpha_1 = -\lim_{\substack{x \rightarrow n_1 \\ x \text{ in } R_2}} T'(x). \quad (6)$$

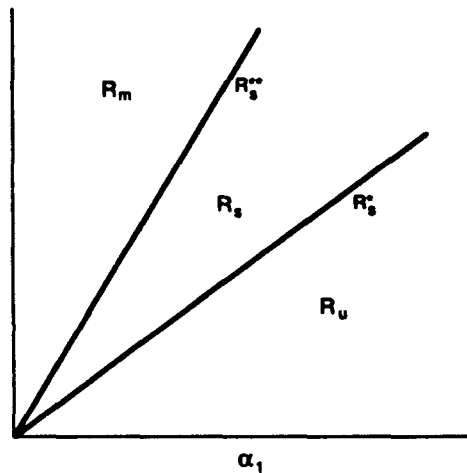


Figure 3. Temperature gradients  $\alpha_1$  and  $\alpha_0$ .

In eq 5,  $L$  is the latent heat of fusion of water,  $b$  is a function of the thickness  $\delta$  of  $R_1$  defined by eq 73c and 73e in Nakano (1990), and  $K_{21}$  is the limiting value of  $K_2$  as  $x$  approaches  $n_1$  when  $x$  is in  $R_1$  and an asterisk denotes that  $K_{21}^*$  is the value of  $K_{21}$  when a point  $(\alpha_1, \alpha_0)$  is on  $R_s^*$  in the diagram of temperature gradients.

In Figure 3 we will refer to the region as  $R_m$  where  $\alpha_0 > (k_1/k_0)\alpha_1, f_{10} < 0$  and an ice layer is melting. The boundary  $R_s^{**}$  is given as

$$\alpha_0 = (k_1/k_0)\alpha_1 \quad \text{on } R_s^{**}. \quad (7a)$$

An existing ice layer neither grows nor melts,  $f_{10}$  vanishes and eq 1 holds true on  $R_s^*$ . The boundary  $R_s^*$  is given as

$$\alpha_0 = k_1(k_0 + LbK_{21}^*)^{-1}\alpha_1 \quad \text{on } R_s^*. \quad (7b)$$

It is easy to see from eq 5 that the steady growth condition of a given soil is uniquely determined by  $\alpha_1$  and  $\alpha_0$ . Nakano (1990) showed that all physical variables such as  $f_{10}$ ,  $T_1$ ,  $\delta$ , etc., are also uniquely determined by  $\alpha_1$  and  $\alpha_0$  for given hydraulic conditions, and applied pressure  $\sigma$ . The hydraulic condition in our tests is specified by the distance  $\delta_0$  between  $n_0$  and  $n$  where the pressure  $P_{1n}$  of water is kept at the atmospheric pressure. Therefore, any point in  $R_s$  is uniquely specified by  $\alpha_1$  and  $\alpha_0$  for given  $\delta_0$ ,  $P_{1n}$  and  $\sigma$ . We will write this as

$$R_s = R_s(\alpha_1, \alpha_0; \delta_0, P_{1n}, \sigma). \quad (8a)$$

Since  $\alpha_1$  and  $\alpha_0$  are related by eq 7b on  $R_s^*$ , any point on  $R_s^*$  is uniquely specified by either  $\alpha_1$  or  $\alpha_0$  for given  $\delta_0$ ,  $P_{1n}$  and  $\sigma$  as

$$R_s^* = R_s^*(\alpha_0; \alpha_1, P_{1n}, \sigma). \quad (8b)$$

The main objective of this work is to show that  $M_1$  is consistent with the data under various applied pressures that were presented in Part I. We will also show that  $M_1$  is consistent with the reported empirical equations such as eq 2a-c and 3b-c. Furthermore, we will evaluate the concept of segregation potential introduced by Konrad and Morgenstern (1980, 1981, 1982) based on  $M_1$  and experimental data.

### PROPERTIES OF $M_1$

Treating a given soil as a mixture of water in liquid phase  $B_1$ , ice  $B_2$  and soil minerals  $B_3$ , Nakano (1990) obtained the exact mathematical solution to the problem of a steadily growing ice layer based on the model  $M_1$  under the following assumptions. The density of each constituent remains constant, the dry density of  $R_0$  remains constant, the part  $R_0$  is kept saturated with water at all times and the pressure of water  $P_{1n}$  at some boundary  $n$  fixed in  $R_0$  remains constant. The thermal conductivity  $k(x)$  in  $R_1$  is assumed to be a nondecreasing linear function of  $x$  given as

$$k(x) = k_0[1 + \eta(x - n_0)], \quad n_1 > x \geq n_0 \quad (9a)$$

$$\eta = (k_{01} - k_0)/(\delta k_0) \quad (9b)$$

$$\lim_{\substack{x \rightarrow n_1 \\ x \text{ in } R_1}} k = k_{01} \leq k_1 \quad (9c)$$

$$\delta = n_1 - n_0. \quad (9d)$$

The temperature  $T$  in  $R_1$  satisfies the equation given as (Nakano, 1990)

$$k(x)T' - c_1 f_{10} T = -k_0 \alpha_0. \quad (10a)$$

The solution of eq 10a is approximately given as

$$T(x) = -\alpha_0 \left[ (x - n_0) + \frac{1}{2} (\beta_0 - \eta) (x - n_0)^2 \right] \quad (10b)$$

$$T_1 = -\alpha_0 a(\delta) \quad (10c)$$

$$T'(n_1^+) = -\alpha_0 b(\delta) \quad (10d)$$

where  $T'(n_1^+)$  is the limiting value of  $T'(x)$  as  $x$  approaches  $n_1$  while  $x$  is in  $R_1$ , and  $a$ ,  $b$  and  $\beta_0$  are defined as

$$a(\delta) = \delta + (1/2) (\beta_0 - \eta) \delta^2 + \dots \quad (11a)$$

$$b(\delta) = (1 + \eta \delta)^{-1} [1 + \beta_0 \delta + \dots] \quad (11b)$$

$$\beta_0 = c_1 f_{10} / k_0. \quad (11c)$$

We derived the following equation of heat balance in  $R_1$  given as

$$k_1 \alpha_1 = k_0 \alpha_0 + (L - c_2 T_1) f_{10} \quad (12)$$

The mass flux of water  $f_{10}$  satisfies the equations (Nakano 1990) given as

$$P_{10} = P_{1n} - [(f_{10} / K_0) + p_0] \delta_0 \quad (13a)$$

$$P_{21} = P_{10} - f_{10} \int_{n_0}^{n_1} K_1^{-1} dx - \int_{n_0}^{n_1} K_1^{-1} K_2 T dx \quad (13b)$$

where  $P_{10} = P_1(n_0)$ ,  $P_{1n} = P_1(n)$

$n$  = some point in  $R_0$

$K_0$  = the hydraulic conductivity in  $R_0$

$p_0$  = gravity term, density  $d_1 \times$  gravitational acceleration

$$\delta_0 = n_0 - n \geq 0. \quad (13c)$$

In order to reduce eq 13b to a simpler form, we introduced (Nakano and Takeda 1991) the following two dimensionless quantities:

$$\phi_0(T) = T^{-1} \int_0^T (K_{10} / K_1) (K_2 / K_{20}) dT \quad (14a)$$

$$\phi_1(T) = T^{-1} \int_0^T (K_{10} / K_1) (k / k_0) dT \quad (14b)$$

where  $K_{10}$  and  $K_{20}$  are the limiting values of  $K_1$  and  $K_2$ , respectively, as  $x$  approaches  $n_0$  while  $x$  is in  $R_1$ . We obtained (Nakano and Takeda 1991) the following equations given as

$$K_0 = K_{10} \quad (15a)$$

$$\gamma = K_{20} / K_0 \quad (15b)$$

$$\phi_{01} = 1, \quad \text{if } f_{10} = 0 \quad (15c)$$

$$-T_1 = (\sigma + \delta_0 K_0^{-1} f_{10}) / I \quad (16a)$$

$$I = \gamma \phi_{01} - K_0^{-1} y \phi_{11} \quad (16b)$$

$$\sigma = P_{21} - P_{1n} \quad (16c)$$

where  $\phi_{01}$ ,  $\phi_{11}$  and  $y$  are defined as

$$\phi_{01} = \phi_0(T_1) \quad (17a)$$

$$\phi_{11} = \phi_1(T_1) \quad (17b)$$

$$y = f_{10}/\alpha_0. \quad (17c)$$

Equation 15a holds true because the composition of the freezing soil is continuous at  $n_0$ , and eq 15b and c follow from eq 4b.

For the sake of convenience we will reduce eq 16a to a form similar to eq 3b. First, we will introduce the following four dimensionless quantities:

$$\omega_0 = \begin{cases} 0, & T_1^{**} = 0 \\ (-T_1^{**})^{-1} \int_0^{T_1^{**}} [1 - K_2(\gamma K_1)^{-1}] dT, & T_1^{**} < 0 \end{cases} \quad (18a)$$

$$\omega_1 = \begin{cases} 1, & T_1 = T_1^{**} \\ (-\Delta T)^{-1} \int_{T_1^{**}}^{T_1} [(K_0 K_2)(K_1 K_{20})^{-1}] dT, & T_1 < T_1^{**} \end{cases} \quad (18b)$$

$$\omega_2 = \begin{cases} 0, & T_1^{**} = 0 \\ (-T_1^{**})^{-1} \int_0^{T_1^{**}} [1 - k K_0 (k_0 K_1)^{-1}] dT, & T_1^{**} < 0 \end{cases} \quad (18c)$$

$$\omega_3 = \begin{cases} 1, & T_1 = T_1^{**} \\ -\Delta T^{-1} \int_{T_1^{**}}^{T_1} k K_0 (k_0 K_1)^{-1} dT, & T_1 < T_1^{**} \end{cases} \quad (18d)$$

Using eq 18a-d, we will write  $\phi_{01}$  and  $\phi_{11}$  as

$$T_1 \phi_{01} = T_1^{**} (1 + \omega_0) - \omega_1 \Delta T \quad (19a)$$

$$T_1 \phi_{11} = T_1^{**} (1 + \omega_2) - \omega_3 \Delta T. \quad (19b)$$

According to M<sub>1</sub> the mass flux of water  $f_{10}$  in a neighborhood of  $n_1$  in  $R_1$  is given as (Nakano and Takeda 1991)

$$f_{10} = -K_{11} P'_1(n_1^+) + b K_{21} \alpha_0 \quad (20)$$

where  $K_{11}$  and  $P'_1(n_1^+)$  are the limiting values of  $K_1$  and  $P'_1$ , respectively, as  $x$  approaches  $n_1$  while  $x$  is in  $R_1$ . We will rewrite eq 20 as

$$y = K_{21} \phi_0 \quad (21a)$$

$$\phi_0 = b - K_{11} P'_1(n_1^+) (\alpha_0 K_{21})^{-1}. \quad (21b)$$

We found (Nakano and Takeda 1991) that  $P'_1(n_1^+)$  is positive in  $R_s$  and vanishes on  $R_s^*$ ; namely

$$P'_1(n_1^+) > 0 \quad \text{in } R_s \quad (22a)$$

$$P'_1(n_1^+) = 0 \quad \text{on } R_s^*. \quad (22b)$$

From eq 22a, 22b and 21b we obtain

$$\varphi_0 = b \quad \text{on } R_s^* \quad (23a)$$

$$b > \varphi_0 > 0 \quad \text{in } R_s \quad (23b)$$

$$\varphi_0 = 0 \quad \text{on } R_s^{**}. \quad (23c)$$

Using eq 21a, we will reduce eq 16b to

$$I = \gamma(\Phi_{01} - \gamma_1 \Phi_0 \Phi_{11}) \quad (24a)$$

where  $\gamma_1$  is defined as

$$\gamma_1 = K_{21} K_{20}^{-1}. \quad (24b)$$

Substituting  $\Phi_{01}$  and  $\Phi_{11}$  in eq 24a by eq 19a and b and using eq 1, we will reduce eq 24a to

$$-T_1 I = \sigma[1 + \omega_0 - \gamma_1 \varphi_0(1 + \omega_2)] + \gamma[\omega_1 - \gamma_1 \varphi_0 \omega_3] \Delta T. \quad (25a)$$

Combining eq 25a with 16a, we obtain

$$\delta_0 K_0^{-1} f_{10} + [\gamma_1 \varphi_0(1 + \omega_2) - \omega_0] \sigma = \gamma[\omega_1 - \gamma_1 \varphi_0 \omega_3] \Delta T. \quad (25b)$$

Now we will reduce eq 25b to a form similar to eq 3b as

$$\Delta T = \hat{a}_0 + \hat{a}_1 f_{10} \quad (25c)$$

where  $\hat{a}_0$  and  $\hat{a}_1$  are defined as

$$\hat{a}_0 = [\gamma_1 \varphi_0(1 + \omega_2) - \omega_0] \sigma (\gamma \varphi_1)^{-1} \quad (25d)$$

$$\hat{a}_1 = \delta_0 (\gamma K_0 \varphi_1)^{-1} \quad (25e)$$

$$\varphi_1 = \omega_1 - \gamma_1 \varphi_0 \omega_3. \quad (25f)$$

We will examine eq 25c for a special case where  $f_{10}$  is very small. It follows from eq 21a that  $\varphi_0$  vanishes as  $f_{10}$  vanishes. We find from eq 18a that  $\omega_0$  vanishes because of eq 4b as  $f_{10}$  vanishes. It follows from eq 1 that  $T_1$  approaches  $T_1^{**}$ ; hence,  $\omega_1$  approaches one as  $f_{10}$  approaches zero. Hence,  $\hat{a}_0$  approaches zero and  $\hat{a}_1$  approaches  $\delta_0 (\gamma K_0)^{-1}$  as  $f_{10}$  approaches zero. Therefore, when  $f_{10}$  is very small, eq 25c may be approximately given as

$$\Delta T = \hat{a}_1 f_{10}. \quad (26)$$

Since  $f_{10}$  is the growth rate of the ice layer, eq 26 states that the growth rate of the ice layer is proportional to the degree of supercooling and that the rate coefficient  $(\hat{a}_1)^{-1}$  depends on the hydraulic properties of  $R_0$  and  $R_1$ , namely the availability of unfrozen water. Equation 26 is consistent with the theory of crystal growth in supercooled liquid (Chalmers 1964).

We will define the thicknesses  $\delta_e$  of  $R_{11}$  and  $\delta^{**}$  of  $R_{10}$  (Fig. 2) as

$$\delta_e = n_1 - n_{10} \quad (27a)$$

$$\delta^{**} = n_{10} - n_0. \quad (27b)$$

Then the thickness  $\delta$  of  $R_1$  is obviously given as

$$\delta = \delta^{**} + \delta_e. \quad (27c)$$

Using eq 10c, we obtain

$$T_1^{**} = -\alpha_0 a (\delta^{**}). \quad (27d)$$

Using eq 10c and 11a, we obtain

$$\Delta T = \alpha_0 a_e \quad (27e)$$

where  $a_e$  is defined as

$$a_e = a(\delta) - a(\delta^{**}) \quad (27f)$$

$$= \delta_e + \frac{1}{2} (\beta_0 - \eta) (\delta_e + 2\delta^{**}) \delta_e + \dots. \quad (27g)$$

Using eq 27e, we will reduce eq 26 to

$$a_e = \hat{a}_1 y \quad (28a)$$

where  $\hat{a}_1$  may be written as

$$\hat{a}_1 = \delta_0 (\gamma K_0)^{-1} (\omega_1 - K_{20}^{-1} \omega_3 y)^{-1}. \quad (28b)$$

When  $f_{10}$  is small,  $y$  and  $\delta_e$  are also small and eq 28a and b are reduced to

$$\delta_e = \hat{a}_1 y \quad (29a)$$

$$\hat{a}_1 = \delta_0 (\gamma K_0 \omega_1)^{-1}. \quad (29b)$$

From eq 29a and b we find that the thickness of the essential frozen fringe is proportional to  $y$  and that the essential frozen fringe vanishes as  $f_{10}$  vanishes. In other words, when  $f_{10}$  is very small, we may state that the appearance of an essential frozen fringe is induced by the flow of unfrozen water regardless of  $\sigma$ . This implies that an essential frozen fringe appears only under a dynamic condition.

## MODEL M<sub>1</sub> AND SEGREGATION POTENTIAL

We will show below that  $M_1$  is consistent with eq 2a, which was found empirically by Konrad and Morgenstern (1980, 1981) and was confirmed by Ishizaki and Nishio (1985). In a typical experiment

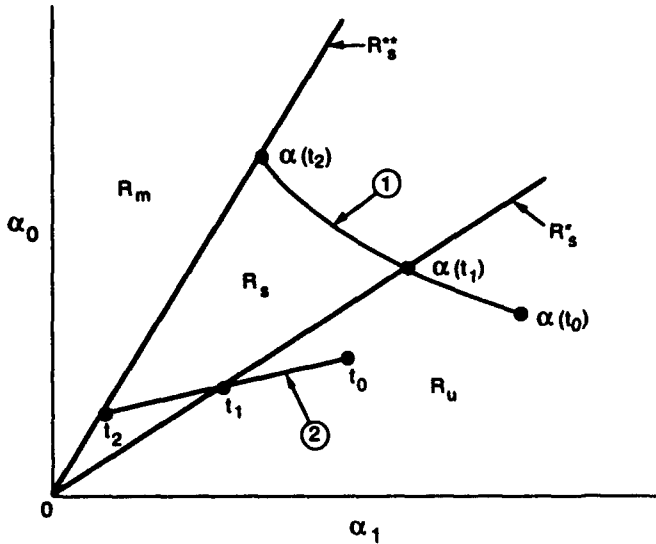


Figure 4. Schematic of trajectories  $\alpha(t)$  that approximately describe the condition of freezing at the formation of the final ice lens.

by Konrad and Morgenstern (1981), the temperature field in the system changes rapidly at the start of the experiment. However, as time elapses, the rate of the change slows down so that the transient freezing may be accurately approximated by a series of successive steady states. Hence, the later part of the experiment can be approximately represented by trajectory 1 in Figure 4, consisting of points  $\alpha(t) = \{\alpha_1(t), \alpha_0(t)\}$  for  $t_2 \geq t \geq t_0$ .

A point  $\alpha(t_0)$  is in  $R_u$  where frozen soil without any visible ice layer grows. As  $\alpha_1$  decreases and  $\alpha_0$  increases, the trajectory approaches the vicinity of a point  $\alpha(t_1)$  in  $R_u$ . As we described previously (Takeda and Nakano 1990) the pattern of ice-rich frozen soil grown in this vicinity evidently depends on the soil type and the magnitude of  $\alpha_1$  (or  $\alpha_0$ ). The results of tests on Kanto loam, for instance, clearly indicate that the pattern of rhythmic ice banding is formed at the small values of  $\alpha_1$  while soil particles or small aggregates of soil particles are evenly dispersed at the greater values of  $\alpha_1$ .

When  $\alpha(t)$  reaches the point  $\alpha(t_1)$  on  $R_u$ , the final ice layer emerges. While  $\alpha(t)$  moves toward the point  $\alpha(t_2)$  on  $R_s^*$ , the growth of the final ice layer continues with the decreasing growth rate until  $\alpha(t)$  reaches the point  $\alpha(t_2)$  on  $R_s^{**}$  where the ice layer stops growing. It should be noted that a line of constant  $f_{10}$  is nearly parallel to  $R_s^*$  because of eq 12. From eq 20 and 22b we obtain on  $R_s^*$

$$f_{10}^* = y^* \alpha_0 = K_{21}^* b \alpha_0 \quad \text{on } R_s^*. \quad (30)$$

It follows from eq 30 that the water intake flux,  $f_{10}^*$ , at the formation of the final ice layer is proportional to the temperature gradient,  $b\alpha_0$ , at  $n_1^+$ . Comparing eq 30 with 2a, we find that  $SP_0$  and  $(T^*)_s$  in eq 2a correspond to  $K_{21}^*$  and  $-b\alpha_0$  in eq 30, respectively. Since the temperature gradient in  $R_1$  does not vary significantly, the segregation potential  $SP_0$  is nothing but  $K_{21}^*$  (the limiting value of the transport function  $K_2$  as  $x$  approaches  $n_1$  while  $x$  is in  $R_1$  at the formation of the final ice layer), when a point  $\alpha(t)$  is on  $R_s^*$  in the diagram of temperature gradients, namely

$$SP_0 = K_{21}^* = y^* b^{-1}. \quad (31)$$

We have shown that  $M_1$  is consistent with eq 2a. It is clear from eq 20 that eq 30 holds true on  $R_s^*$  but does not hold in  $R_s$  because of eq 22a. In other words, the value of  $y$  defined by eq 17c is equal to  $bK_{21}^*$  on  $R_s^*$ . However, the value of  $y$  in  $R_s$  depends on a specific trajectory  $\alpha(t)$ . For instance, on trajectory 1 in Figure 4 the value of  $y$  decreases from  $bK_{21}^*$  as  $\alpha(t)$  moves toward the point  $\alpha(t_2)$  from the point  $\alpha(t_1)$  and vanishes at the point  $\alpha(t_2)$ . On this trajectory  $f_{10}$  decreases with the increasing  $\alpha_0$ . However, it is easy to see that  $f_{10}$  decreases with the decreasing  $\alpha_0$  on trajectory 2 for  $t_2 > t > t_1$ . Therefore,  $M_1$  is also consistent with the empirical finding by Ishizaki and Nishio (1985) that the value of  $y$  varies

widely and that  $f_{10}$  may either increase or decrease with the increasing  $\alpha_0$  depending on a given specific trajectory. This finding by Ishizaki and Nishio (1985) was empirically confirmed (Nakano and Takeda 1991) when  $\sigma = 0$ .

According to our definition  $K_{21}^*$  is the value of  $K_{21}$  evaluated on  $R_s^*$ . Since any point on  $R_s^*$  is uniquely specified by eq 8b, we may write  $K_{21}^*$  as

$$K_{21}^* = K_{21}^*(\alpha_0; \delta_0, P_{1n}, \sigma). \quad (32)$$

We studied (Nakano and Takeda 1991) the dependence of  $K_{21}^*$  on  $\alpha_0$  for a special case where  $\delta_0 = 2.0$  cm,  $P_{1n} = 0.1$  MPa and  $\sigma = 0$  for three types of soils. It was found that  $K_{21}^*$  is nearly constant for a soil if  $\alpha_0$  is greater than  $2.0$  ( $^{\circ}\text{C cm}^{-1}$ ). However,  $K_{21}^*$  tends to increase with decreasing  $\alpha_0$  in the range of  $\alpha_0$  with  $2.0$  ( $^{\circ}\text{C cm}^{-1}$ )  $> \alpha_0 > 0$  for the two types of soils, Tomakomai silt and Fujinomori. Unfortunately, we were unable to confirm behavior similar to this of  $K_{21}^*$  for Kanto loam because of a lack of data. Using the additional data newly obtained, we will show such behavior for Kanto loam below.

Konrad and Morgenstern (1980, 1981, 1982) empirically found eq 2b that is equivalent to the following equation given as

$$K_{21}^* = K_{21}^*(P_{10}^*, \sigma) \quad (33)$$

where an asterisk for  $P_{10}$  is used to emphasize that the value of  $P_{10}$  is evaluated when a point  $\alpha(t)$  is on  $R_s^*$ . Since their hydraulic conditions were not specified in the same manner as in our experiments, we will reduce eq 33 to the form appropriate to our system. In our system  $P_{10}$  is given by eq 13a. Hence, we obtain

$$P_{10}^* = P_{1n} - \left[ \left( f_{10}^* / K_0 \right) + p_0 \right] \delta_0 \quad (34)$$

where  $f_{10}^*$  is the value of  $f_{10}$  on  $R_s^*$  and is uniquely determined by  $\alpha_0$  (eq 8b) if  $\delta_0, P_{1n}$  and  $\sigma$  are given. Therefore,  $P_{10}^*$  in eq 33 can be replaced by  $\alpha_0, \delta_0$  and  $P_{1n}$  so that eq 33 is reduced to eq 32. We have shown that  $M_1$  is consistent with eq 2b, which was found empirically by Konrad and Morgenstern (1980, 1981, 1982).

Konrad and Morgenstern (1981) empirically found that  $SP_0$  is a monotonically decreasing function of  $-P_{10}^*$  when  $\sigma = 0$ . Since  $P_{10}^*$  represents the combined effects of  $\alpha_0, \delta_0$  and  $P_{1n}$ , in order to find the effect of the temperature gradient, we plotted the data of  $SP_0$  vs.  $(-T')_a$  obtained by Konrad and Morgenstern (1981) in Figure 5, where the number assigned to each data point corresponds to the test number of their E series experiments. The data points E4 through 7 were obtained for a single layer of Devon silt under various temperature conditions. These data points clearly indicate that  $SP_0$  tends to increase with the decreasing temperature gradient. This tendency is consistent with our empirical findings. Tests E8 and E9 were both two-layer systems in which the hydraulic conductivities  $K_0$  of the unfrozen bottom layers were, respectively, higher and lower than that

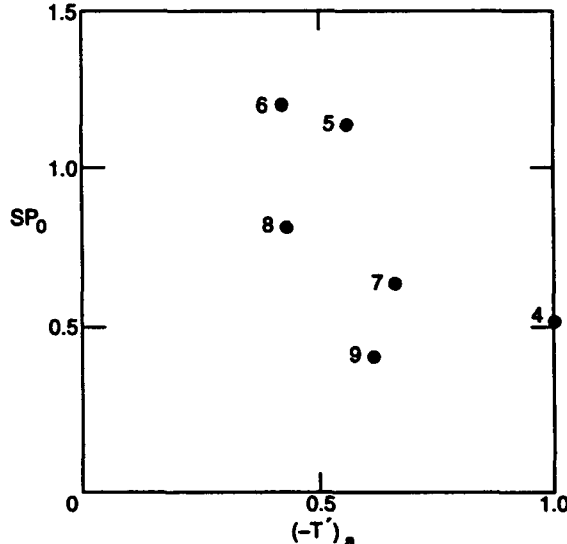


Figure 5. Values of  $SP_0$  [ $\text{g}(\text{cm } ^{\circ}\text{C } \text{d})^{-1}$ ] vs. the values of the average temperature gradient  $(-T')_a$  ( $^{\circ}\text{C cm}^{-1}$ ) obtained by Konrad and Morgenstern (1981).

of the unfrozen Devon silt. Since the temperature gradients in these two tests were not equal, the effects of hydraulic conditions alone on  $SP_0$  are difficult to assess.

## RESULTS OF DATA ANALYSIS

### Steady growth condition

We will examine the validity of the model  $M_1$  under the applied pressure by using the experimental data presented in Part I (Takeda and Nakano 1993). We found empirically that the steady growth region  $R_s(\sigma)$  under a given applied pressure  $\sigma$  is approximately described as

$$\alpha_u = A\alpha_i, \quad k_1 k_0^{-1} > A > S(\sigma) \quad (35)$$

where  $\alpha_u$  = absolute value of the temperature gradient near  $n_0$  in  $R_0$

$\alpha_i$  = absolute value of the temperature gradient near  $n_1$  in  $R_1$

$S$  = property of a given soil that depends on the applied pressure  $\sigma$ .

The temperature profiles in the frozen and the unfrozen parts are not exactly linear when the steady growth of an ice layer is taking place because of the convective heat transport. However, the amount of heat transported by convection is much less than that transported by conduction. The difference between  $\alpha_u$  (or  $\alpha_i$ ) and  $\alpha_0$  (or  $\alpha_1$ ) is negligibly small as shown empirically and theoretically in Nakano and Takeda (1991). Therefore, eq 35 is nearly equivalent to

$$\alpha_0 = A\alpha_1, \quad -k_1 k_0^{-1} > A > S(\sigma). \quad (36)$$

We will no longer discriminate  $\alpha_u$  (or  $\alpha_i$ ) from  $\alpha_0$  (or  $\alpha_1$ ) in the following discussion.

According to  $M_1$  the steady growth region  $R_s(\sigma)$  under a given applied pressure  $\sigma$  is given by eq 5. Using  $y^*$ , we will reduce eq 5 to a form similar to eq 36 as

$$\alpha_0 = A\alpha_1, \quad k_1 k_0^{-1} > A > k_1 (k_0 + Ly^*)^{-1}. \quad (37)$$

Comparing eq 37 with 36, we find that  $M_1$  is consistent with the experimental data if the following relation holds:

$$S(\sigma) \geq k_1 [k_0 + Ly^*(\sigma)]^{-1}. \quad (38a)$$

We will define  $\bar{y}^*$  as

$$S(\sigma) = k_1 [k_0 + L\bar{y}^*(\sigma)]^{-1}. \quad (38b)$$

Then, it is easy to see that eq 38a is equivalent to the following relation:

$$y^*(\sigma) \geq \bar{y}^*(\sigma). \quad (38c)$$

We will examine the validity of eq 38c below.

For a given  $\sigma$  the value of  $y^*(\sigma)$  can be calculated by using the calculated value of  $f_{10}$  based on either the measured rate of heave  $r$  or the measured rate of water intake, and the measured value of  $\alpha_0$  at each data point  $(\alpha_i, \alpha_0)$  on  $R_s^*$ . The calculated values of  $y^*(\sigma)$  are plotted vs.  $\alpha_0$  with  $\sigma$  being a parameter in Figure 6. The mass flux of water  $f_{10}$  decreases by the order of  $10^{-2}$  as  $\sigma$  increases from zero to 195 kPa. As the result the accuracy of measuring  $f_{10}$  tends to decrease with increasing  $\sigma$  and the variability of data points becomes more pronounced with increasing  $\sigma$ , as shown in Figure 6.

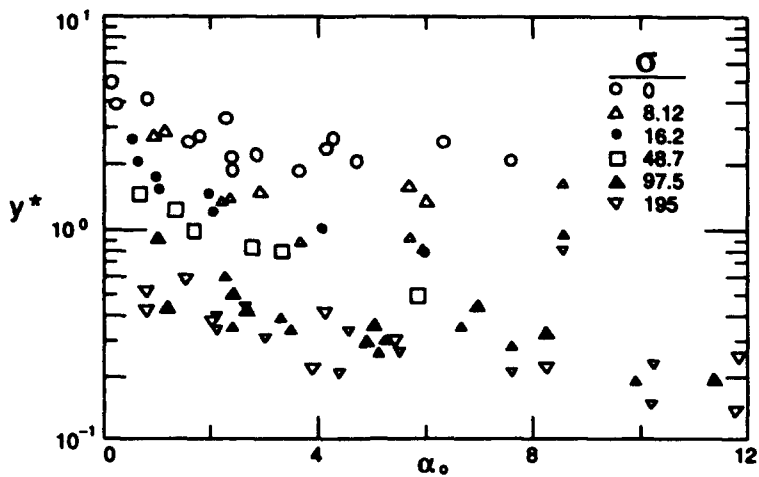


Figure 6. Values of  $y^*$  [ $\text{g}(\text{cm} \text{ } ^\circ\text{C} \text{ } \text{d})^{-1}$ ] vs.  $\alpha_0$  under various applied pressures  $\sigma$  (kPa).

Because of such variability and the limited numbers of data under  $\sigma = 390$  kPa, we decided not to use the data taken under  $\sigma = 390$  kPa in our analysis. From Figure 6 we find the general trend that  $y^*$  decreases with increasing  $\sigma$  and that  $y^*$  increases with the decreasing  $\alpha_0$  in the range of  $\alpha_0 < 2.0 \text{ } ^\circ\text{C} \text{ } \text{cm}^{-1}$ . The latter trend was also observed (Nakano and Takeda 1991) in the experiments with Tomakomai silt and Fujinomari clay under null applied pressure.

We calculated the values of  $\bar{y}^*(\sigma)$  from the values of  $S(\sigma)$  that were presented in Table 2 of Part I (Takeda and Nakano 1993). We also calculated the average of  $y^*(\sigma)$  over all the data points obtained for each  $\sigma$ . The values of  $\bar{y}^*(\sigma)$  and the average values  $y_a^*(\sigma)$  of  $y^*(\sigma)$  for each  $\sigma$  are presented in Table 1. It is clear from Table 1 that eq 38c does not hold for every  $\sigma$ , particularly for greater values of  $\sigma$ . However, the average values  $y_a^*(\sigma)$  do not differ significantly from those of  $y^*(\sigma)$ . We may conclude that the model  $M_1$  is consistent with the experimental data regardless of  $\sigma$  and that the steady growth region of an ice layer under various applied pressures can be described by eq 37.

In order to find the dependence of  $y_a^*$  on  $\sigma$ , we plotted  $y_a^*$  in the logarithmic scale against  $\sigma$  in Figure 7. It is clear from the figure that  $y_a^*$  is a decreasing function of  $\sigma$ . Assuming that  $b$  is nearly equal to one, we may conclude that  $K_{21}^*$  (or  $SP_0$ ) is a decreasing function of  $\sigma$ , which was found

Table 1. Calculated values  $\bar{y}^*$  [ $\text{g}(\text{cm} \text{ } ^\circ\text{C} \text{ } \text{d})^{-1}$ ] and the average measured values  $y_a^*$  under various applied pressures  $\sigma$  (kPa).

Applied pressures ( $\sigma$ )					
0.0	8.12	16.2	48.7	97.8	195
2.34	2.12	1.14	1.12	0.72	0.56
2.86	1.98	1.61	0.97	0.45	0.35

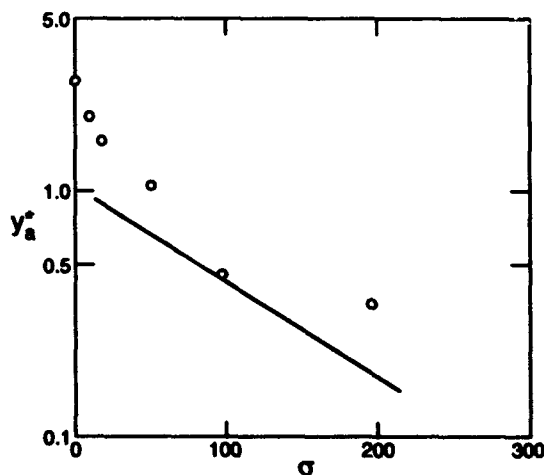


Figure 7. Average values  $y_a^*$  [ $\text{g}(\text{cm} \text{ } ^\circ\text{C} \text{ } \text{d})^{-1}$ ] vs.  $\sigma$  (kPa) where a solid line is the empirically determined relationship for Devon silt obtained by Konrad and Morgenstern (1982).

empirically by Konrad and Morgenstern (1982). Their data with Devon silt were presented in the functional form given as

$$SP_0 = a_2 \exp(-a_3 \sigma). \quad (39)$$

When we use the same units of  $SP_0$  and  $\sigma$  as those of  $y^*$  and  $\sigma$  in Figure 7, the values of the constants  $a_2$  and  $a_3$  are 1.04 and  $8.95 \times 10^{-3}$ , respectively, and eq 39 is presented by the straight line in Figure 7. Because of the limited number of data points it is not certain that our data can be presented in the same functional form as eq 39. However, the important point is that  $K_{21}^*$  is a decreasing function of  $\sigma$ . The reason for such dependence will be discussed below.

### Dependence of $y^*$ on $T_1^*$

Combining eq 30 with eq 32, we obtain

$$y^* = b K_{21}^* (\alpha_0, \delta_0, P_{1n}, \sigma). \quad (40a)$$

For a special case such as our experiments where  $\delta_0$  and  $P_{1n}$  are specified, we may reduce eq 40a to:

$$y^* = b K_{21}^* (\alpha_0, \sigma). \quad (40b)$$

On the other hand  $K_{21}^*$  is the value of  $K_{21}$  when a point  $(\alpha_1, \alpha_0)$  is on  $R_s^*$ . From eq 4e we obtain

$$K_{21}^* = K_{21}(T_1^*, \rho) \quad (40c)$$

where  $T_1^*$  is the temperature at  $n_1$  when a point  $(\alpha_1, \alpha_0)$  is on  $R_s^*$ . It is clear from eq 40b and c that  $T_1^*$  and the composition  $\rho$  generally depend on  $\alpha_0$  and  $\sigma$ . We will study empirically the relationship between  $y^*$  and  $T_1^*$  below.

Using the set of data obtained under the applied pressure of 48.7 kPa as an example, we will describe how we obtained the empirically determined value of  $T_1^*$  from the data. The results of our data analysis are presented in Table 2, where  $n_1$  is the observed location of the interface between  $R_1$  and  $R_2$ , while  $n_0$  is the location of the 0°C isotherm calculated by using the measured temperature profile in  $R_0$ . The values of  $\delta$  in the table are calculated simply from eq 9d and vary between 0.91 and 1.5 mm. We have found that the value of  $\delta$  increases with the increasing  $\sigma$  and that the maximum value of  $\delta$  in the range of  $\sigma \leq 195$  kPa is 4.8 mm under the condition of  $\alpha_0 = 0.80$  and  $\sigma = 195$  kPa.

The value of  $T_1^*$  can be calculated from either the measured temperature profile in  $R_0$  or that in  $R_2$ . As we discussed in Part I (Takeda and Nakano 1993), the temperature measurements in  $R_0$  are more accurate than those in  $R_2$ . Therefore, it is desirable to determine  $T_1^*$  from the profile in  $R_0$ . However, the thermal conductivity  $k(x)$  in  $R_1$  is unknown because the composition of  $R_1$  is unknown. According to the model  $M_1$ ,  $T_1$  is given by eq 10c and 11a. Hence, when the variation of  $k$  in  $R_1$  is small,  $T_1^*$  is nearly equal to  $T_{10}$  defined as

Table 2. Summary of data analysis with  $\sigma = 48.7$  kPa.

Exp.	$\alpha_0$ (°C cm <sup>-1</sup> )	$f_{10}$ (g cm <sup>-2</sup> d <sup>-1</sup> )	$y^*$ lg (cm °C d <sup>-1</sup> )	$n_1$ (cm)	$n_0$ (cm)	$\delta$ (cm)	$-T_{10}$ (°C)	$-T_{11}$ (°C)	$\hat{T}_1^*$ (°C)
1	0.642	0.968	1.51	0.67	0.55	0.12	0.076	0.174	0.125
2	1.29	1.59	1.23	0.25	0.099	0.15	0.192	0.198	0.195
3	1.62	1.60	0.988	0.28	0.13	0.15	0.239	0.211	0.225
4	2.76	2.13	0.770	0.18	0.086	0.094	0.260	0.245	0.255
5	3.29	2.65	0.804	0.20	0.080	0.12	0.378	0.320	0.349
6	5.85	2.97	0.507	0.13	0.039	0.091	0.535	0.467	0.501

$$T_{10} = -\alpha_0 \delta. \quad (41a)$$

It is clear from eq 10c and 11a that  $T_1^*$  is accurately approximated also by  $T_{10}$  when  $\delta$  is very small. The calculated values of  $T_{10}$  are listed in Table 2. When  $\sigma$  is negligible, Nakano and Takeda (1991) found that  $k(x)$  tends to increase with  $x$  in  $R_1$ . Therefore,  $T_{10}$  would be a lower bound of  $T_1^*$ , namely

$$T_1^* \geq T_{10}. \quad (41b)$$

We also calculated the value of  $T_1^*$  from the measured profile in  $R_2$ . The calculated values, which are referred to as  $T_{11}$ , are listed in Table 2. We find from Table 2 that  $T_{10}$  tends to be less than  $T_{11}$ . A tendency similar to this was also found in all other cases of different applied pressures. Under these circumstances we decided to choose the average of  $T_{10}$  and  $T_{11}$  to be the empirically determined value  $\hat{T}_1^*$  of  $T_1^*$  defined as

$$\hat{T}_1^* = 0.5 (T_{10} + T_{11}). \quad (42)$$

The values of  $\hat{T}_1^*$  are listed in Table 2.

The values of  $y^*$  are plotted against  $-\hat{T}_1^*$  with the logarithmic scale under various applied pressures  $\sigma$  in Figure 8. Despite some scatter, it is clear that the relation between  $y^*$  and  $-\hat{T}_1^*$  is nearly one to one. The solid line in Figure 8 is the best linear approximation to the data points given as

$$y^* = K_{21}^* = \begin{cases} K_{20} & \hat{T}_0 < T \leq 0 \\ K_{20}(\hat{T}_0/T)^{b_2} & T \leq \hat{T}_0 \end{cases} \quad (43a)$$

$$T \leq \hat{T}_0 \quad (43b)$$

where  $b$  is assumed to be one,  $K_{20}$  is the limiting value of  $K_2$  as  $x$  approaches  $n_0$  while  $x$  is in  $R_1$  and is equal to  $1.98 \times 10^3 \text{ g}(\text{cm} \text{ }^\circ\text{C})^{-1}$  (Nakano and Takeda 1991),  $\hat{T}_0 = -1.5 \times 10^{-4} \text{ }^\circ\text{C}$  and  $b_2 = 1.039$ . As we showed (Nakano and Takeda 1991),  $K_{20}$  satisfies the equation given as

$$K_{20} = \gamma K_0 \quad (44)$$

where  $K_0$  is the hydraulic conductivity in  $R_0$ . It is easy to see that  $y^*$  becomes infinite as  $T$  approaches zero in eq 43b. Although eq 43b is the best approximation to the data points, eq 43a is needed to fit the data points in a neighborhood of  $T = 0^\circ\text{C}$ .

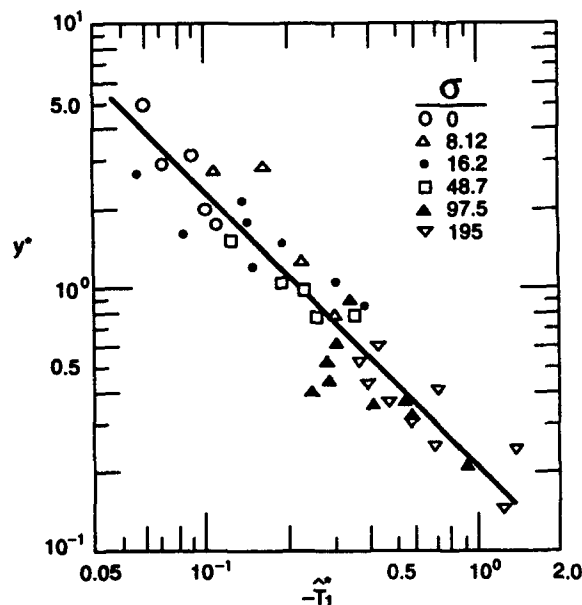


Figure 8. Values of  $y^*$  [ $\text{g}(\text{cm} \text{ }^\circ\text{Cd})^{-1}$ ] vs. the temperature  $-\hat{T}_1^*$  ( $^\circ\text{C}$ ) under various applied pressures  $\sigma$  (kPa).

According to eq 40c,  $y^*$  generally depends on  $T_1^*$  and the composition  $\rho$ . However, we have found empirically that  $y^*$  depends mainly on  $T_1^*$ . This implies that the composition in a neighborhood of  $n_1$  in  $R_1$  is not significantly affected by  $\sigma$  and  $\alpha_0$  (or  $f_{10}$ ). Since  $\hat{T}_1^*$  varies between 0 and  $-1.0^\circ\text{C}$  in Figure 8, we may conclude that the composition of the essential frozen fringe  $R_{11}$  depends mainly on the temperature regardless of  $\sigma$  and  $f_{10}$ . There is another interpretation of Figure 8: that the transport function  $K_2$  does not depend on the composition. Recently Nakano and Tice (1990) found empirically that  $K_2$  in unsaturated frozen clay strongly depends on the composition, particularly the content of ice. Their empirical finding supports the former interpretation.

Figure 8 shows that the range of  $\hat{T}_1^*$  for a given  $\sigma$  shifts toward the lower temperature as  $\sigma$  increases. The segregation potential  $K_{21}^*$  evidently depends primarily on the temperature  $T_1^*$  at  $n_1$  and is an increasing function of  $T_1^*$  because the applied pressure in the range of  $\sigma \leq 195 \text{ kPa}$  does not affect significantly the composition of the essential frozen fringe  $R_{11}$ . This is the reason why the segregation potential  $K_{21}^*$  is generally a decreasing function of  $\sigma$ .

#### Dependence of $T_1^*$ on $f_{10}^*$

The values of  $-\hat{T}_1^*$  are plotted against  $f_{10}^*$  under various applied pressures  $\sigma$  in Figure 9. Figure 9 shows that the relationship between  $\hat{T}_1^*$  and  $f_{10}^*$  is approximately linear for a given  $\sigma$ , which is consistent with the empirical relation (eq 3b and c) found by Ishizaki and Nishio (1985). It is clear from Figure 9 that the constants  $a_0$  and  $a_1$  strongly depend on  $\sigma$ . An important question is whether we can describe the behavior of data points in Figure 9 by eq 25c derived based on  $M_1$ . We are not able to show that eq 25c is consistent with the data because we have no data on the transport function  $K_1$ . However, we will show below that eq 25c is consistent with the data if the function  $K_1$  is properly chosen.

The model  $M_1$  is defined as the frozen fringe where ice may exist but does not grow, and the mass flux of water  $f_1$  is given by eq 4a with the condition of eq 4b and c. When  $\sigma > 0$ , the essential frozen fringe  $R_{11}$  vanishes as  $f_1$  vanishes but  $R_{10}$  does not. From eq 4b we obtain:

$$K_2/K_1 = \gamma \quad \text{in } R_{10} \text{ if } f_1 = 0. \quad (45)$$

When the steady growth of an ice layer occurs,  $f_1$  remains constant at  $f_{10}$  throughout  $R_0$ ,  $R_{10}$  and  $R_{11}$ . An important question arises: whether or not eq 45 holds true when  $f_{10}$  does not vanish. In other

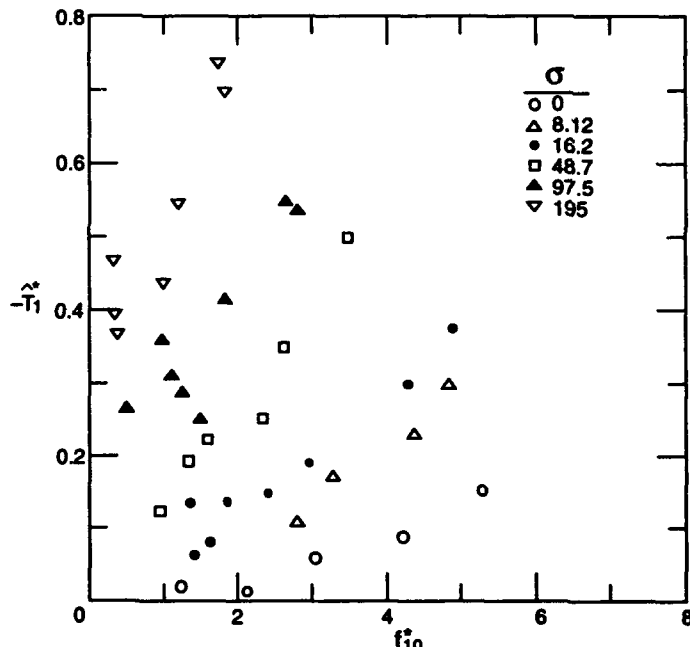


Figure 9. Values of  $-\hat{T}_1^*$  ( $^\circ\text{C}$ ) vs. the mass flux of water  $f_{10}^*$  [ $\text{g}(\text{cm}^{-2}\text{d}^{-1})$ ] under various applied pressures  $\sigma$  (kPa).

words, is the composition of  $R_{10}$  significantly affected by  $f_{10}$ ? As we described above, our data indicate that neither  $\sigma$  nor  $f_{10}$  significantly affects the composition of the essential frozen fringe. Therefore, it is probable that the effect of  $f_{10}$  on the composition of  $R_{10}$  is negligible. We will assume that eq 45 holds true regardless of  $f_{10}$ , namely

$$K_2/K_1 = \gamma \quad \text{in } R_{10} \quad (46)$$

When eq 46 holds true, the dimensionless quantity  $\omega_0$  defined by eq 18a vanishes. Hence, eq 25d is reduced to

$$\hat{a}_0 = \gamma_1 \varphi_0 (1 + \omega_2) \sigma (\gamma \varphi_1)^{-1}. \quad (47)$$

Now we will calculate  $T_1^*$  as a function of  $f_{10}^*$  by eq 25c as follows. Since  $T_1^*$  is the value of  $T_1$  on  $R_1^*$ ,  $\varphi_0$  is equal to  $b$  by eq 23a. We will assume that  $b = 1$ , or equivalently  $k(x) = k_0$  in  $R_1$ . We also assume that  $K_2(T)$  is equal to  $K_2^*(T)$  given by eq 43a and b. The value of  $T_1^{**}$  is calculated by eq 1 for a given  $\sigma$ . Horiguchi and Miller (1983) found empirically that the transport functions  $K_1(T)$  of various soils can accurately be represented in the same functional form as eq 43b. We will assume that  $K_1(T)$  is given as

$$K_1(T) = \begin{cases} K_0 & \hat{T}_0 < T \leq 0 \\ K_0 (\hat{T}_0/T)^{b_1} & T \leq \hat{T}_0 \end{cases} \quad (48)$$

where  $K_0$  is the hydraulic conductivity in  $R_0$  and is  $1.77 \times 10^3 \text{ g(cm d MPa)}^{-1}$  (Nakano and Takeda 1991). The value of  $\hat{T}_0$  is the same as used in eq 43a and b. A constant  $b_1$  is an unknown parameter to be determined.

As we described in Part I (Takeda and Nakano 1993), the applied pressure  $\sigma$  affects the void ratio  $e$  of a specimen. Although the variation of  $e$  itself is negligibly small, the hydraulic conductivity  $K_0$  may be affected significantly. Therefore, we determined empirically the relationship between  $K_0$  and  $\sigma$  given as

$$K_0(\sigma) = 1.77 \times 10^3 \sigma^{-0.1068} \quad (49)$$

where the units of  $K_0$  and  $\sigma$  are  $\text{g(cm d MPa)}^{-1}$  and  $\text{kPa}$ , respectively. The value of  $K_0$  is reduced to about one-half according to eq 49 when  $\sigma$  is increased from zero to 195 kPa. The functional form of eq 49 is consistent with the data obtained by Fukushima and Ishii (1986). In our calculations of  $T_1^*$  for  $\sigma > 0$  we used  $K_0(\sigma)$  given by eq 49 instead of the value of  $K_0$  at  $\sigma = 0$ .

Now we can calculate  $T_1^*(f_{10})$  with  $b_1$  being a parameter. Calculating  $T_1(f_{10})$  in the wide range of  $b_1$ , we find that the calculated curves  $T_1^*(f_{10})$  fit the data well if  $b_1$  is about one-half of  $b_2$ . The calculated curves with  $b_1 = 0.52$  are presented in Figure 10 together with the data. If  $b_1$  is decreased (or increased) from this value, then the gradients of these curves,  $d(-T_1^*)/df_{10}^*$  increase (or decrease). We have shown that eq 25c is consistent with the data if the function  $K_1$  is given by eq 48 with  $b_1 = 0.52$ .

## DISCUSSION AND CONCLUSIONS

Many models of frost heave have been proposed in the past (Nakano 1990). However, the model proposed by Konrad and Morgenstern (1982) is one of few that were built on an empirical base. Their segregation potential theory was easily adapted to solve engineering problems in the past. As our quantitative understanding on the subject is increased, their model can be improved or refined without sacrificing its easy adaptability to engineering problems.

Konrad and Morgenstern (1981) proposed an equation similar to eq 4a where the mass flux of water  $f_1$  is given as the sum of two terms, namely, a pressure-related term and a temperature related

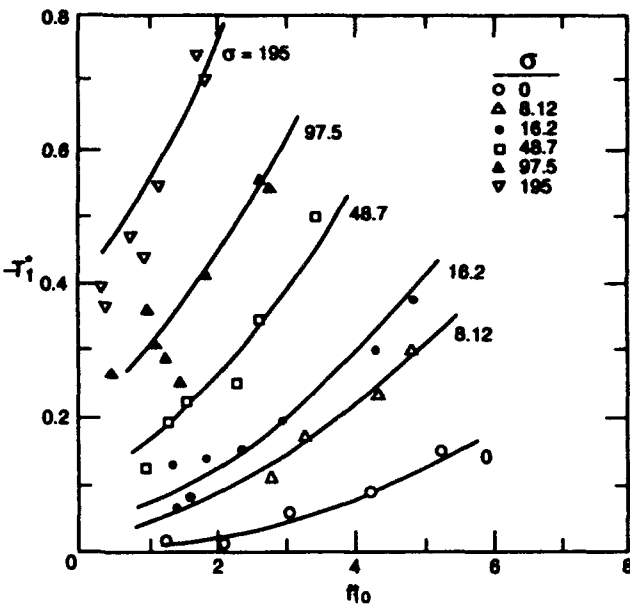


Figure 10. Values of  $-\hat{T}_1$  ( $^{\circ}$ C) vs. the flux  $f_{10}^*$  ( $cm^{-2} d^{-1}$ ) where solid curves are predicted relationships between these two variables by eq 25c under various applied pressures  $\sigma$  (kPa).

term. However, curiously enough, they dropped the pressure term in their later publications. Since the pressure term in eq 4a is generally negative according to  $M_1$ , the omission of this term leads to overestimating  $f_1$ . Therefore, their model certainly predicts an upper bound of frost heave as they claim (Konrad and Morgenstern 1982). However, some serious criticisms against their model cannot be refuted unless the pressure term is restored, as we will explain below.

When the pressure term is neglected, it is clear from eq 4a that  $f_1$  is nonnegative. This is the reason why Konrad and Morgenstern (1982) could not provide a satisfactory explanation for the expulsion of water from freezing soils. Takashi et al. (1978) conducted a series of frost heave tests in which the temperature in the unfrozen part  $R_0$  was kept constant at 0.2–0.3°C higher than the freezing point of specimens. In other words, the positive temperature term of eq 4a was kept small in their tests.

The absolute value of the negative pressure term of eq 4a is small when the applied pressure  $\sigma$  is small. Hence,  $f_1$  can be positive when  $\sigma$  is small. However, the pressure term decreases with the increasing  $\sigma$  and  $f_1$  vanishes at certain values of  $\sigma$  because the two terms of eq 4a cancel out. As  $\sigma$  increases beyond this value,  $f_1$  becomes negative; that is, the expulsion of water from freezing soils takes place. Takashi et al. (1978) found empirically what we described above.

Another serious criticism of the segregation potential theory was raised by Ishizaki and Nishio (1985) that the value of  $y_s$  defined by eq 3a is constant strictly at the instant when the final ice lens emerges, but except for this instant,  $y_s$  varies widely during the growth period of the final ice lens. As we explained earlier, the pressure term of eq 4a vanishes at the formation of the final ice lens, but the negative pressure term varies depending on a specific trajectory in the diagram of temperature gradients when the final ice lens is growing. The empirical finding by Ishizaki and Nishio (1985) can be explained if the pressure term is restored. Assuming that the temperature  $T_1^*(\sigma)$  at the formation of the final ice lens depends mainly on the property of a given soil alone, Konrad and Morgenstern (1982) termed  $T_1^*(\sigma)$  as the "segregation freezing temperature." However, we have found empirically (Fig. 9) that  $T_1^*(\sigma)$  depends strongly on the mass flux  $f_{10}^*$ .

Using the data obtained in Part I (Takeda and Nakano 1993), we evaluated the accuracy of  $M_1$ . We found that the predicted steady growth condition of an ice layer under various applied pressures is in good agreement with that found empirically. We also found that  $M_1$  is consistent with the data obtained by Konrad and Morgenstern (1980, 1981, 1982) that were used to support their segregation potential theory. Their method of frost heave prediction is a sound and useful tool for engineering problems that consistently provides an upper bound of frost heave. However, the accuracy of their method can be significantly improved and some of the serious criticisms against it can be refuted if the pressure term in the equation of water flow is restored as we discussed above.

## LITERATURE CITED

Chalmers, B. (1964) *Principles of Solidification*. New York: John Wiley & Sons.

Edlefsen, N.E. and A.B.C. Anderson (1943) Thermodynamics of soil moisture. *Hilgardia*, 15(2): 31-298.

Fukushima, S. and T. Ishii (1986) An experimental study of the influence of confining pressure on permeability coefficients of fill dam core material. *Japanese Society of Soil Mechanics and Foundations Engineering*, 26: 32-46.

Horiguchi, K. and R.D. Miller (1983) Hydraulic conductivity functions of frozen materials. In *Proceedings, 4th International Conference on Permafrost, July 17-22, Fairbanks, Alaska*. Washington, D.C.: National Academy Press, p. 504-508.

Ishizaki, T. and N. Nishio (1985) Experimental study of final ice lens growth in partially frozen saturated soil. In *Proceedings, 4th International Symposium on Ground Freezing, 5-7 August, Sapporo, Japan* (S. Kinoshita and M. Fukuda, Ed.). Rotterdam, Netherlands: A.A. Balkema, p. 71-78.

Konrad, J.M. and N.R. Morgenstern (1980) A mechanistic theory of ice lens formation in fine-grained soils. *Canadian Geotechnical Journal*, 17: 473-486.

Konrad, J.M. and N.R. Morgenstern (1981) The segregation potential of a freezing soil. *Canadian Geotechnical Journal*, 18: 482-491.

Konrad, J.M. and N.R. Morgenstern (1982) Effects of applied pressure on freezing soils. *Canadian Geotechnical Journal*, 19: 494-505.

Nakano, Y. (1990) Quasi-steady problems in freezing soils: I. Analysis on the steady growth of an ice layer. *Cold Regions Science and Technology*, 17(3): 207-226.

Nakano, Y. and K. Takeda (1991) Quasi-steady problems in freezing soils: III. Analysis on experimental data. *Cold Regions Science and Technology*, 19: 225-243.

Nakano, Y. and A.R. Tice (1990) Transport of water due to a temperature gradient in unsaturated frozen clay. *Cold Regions Science and Technology*, 18: 57-75.

Radd, F.J. and D.H. Oertle (1973) Experimental pressure studies of frost heave mechanism and the growth-fusion behavior of ice. In *Permafrost: The North American Contribution to the 2nd International Conference on Permafrost, Yakutsk, 13-28 July*. Washington, D.C.: National Academy of Sciences, p. 377-384.

Takashi, T., H. Yamamoto, T. Ohrai and M. Masuda (1978) Effect of penetration rate of freezing and confining stress on the frost heave ratio of soil. In *Proceedings, 3rd International Conference on Permafrost, 10-13 July, Edmonton, Alberta*. Ottawa: National Research Council of Canada, vol. 1, p. 737-742.

Takashi, T., T. Ohrai, H. Yamamoto and J. Okamoto (1981) Upper limit of heaving pressure derived by pore-water pressure measurements of partially frozen soil. *Engineering Geology*, 18: 245-257.

Takeda, K. and Y. Nakano (1990) Quasi-steady problems in freezing soils: II. Experiment on steady growth of an ice layer. *Cold Regions Science and Technology*, 18: 225-247.

Takeda, K. and Y. Nakano, Y. (1993) Growth condition of an ice layer in frozen soils under applied loads: I. Experiment. USA Cold Regions Research and Engineering Laboratory, CRREL Report 93-21.

# REPORT DOCUMENTATION PAGE

Form Approved  
OMB No. 0704-0188

Public reporting burden for this collection of information is estimated to average 1 hour per response, including the time for reviewing instructions, searching existing data sources, gathering and maintaining the data needed, and completing and reviewing the collection of information. Send comments regarding this burden estimate or any other aspect of this collection of information, including suggestion for reducing this burden, to Washington Headquarters Services, Directorate for Information Operations and Reports, 1215 Jefferson Davis Highway, Suite 1204, Arlington, VA 22202-4302, and to the Office of Management and Budget, Paperwork Reduction Project (0704-0188), Washington, DC 20503.

1. AGENCY USE ONLY (Leave blank)	2. REPORT DATE January 1994	3. REPORT TYPE AND DATES COVERED
4. TITLE AND SUBTITLE  Growth Condition of an Ice Layer in Frozen Soils Under Applied Loads 2. Analysis		5. FUNDING NUMBERS  PE: 6.11.02A PR: 4A161102AT24 TA: SC WU: F01
6. AUTHORS  Yoshisuke Nakano and Kazuo Takeda		
7. PERFORMING ORGANIZATION NAME(S) AND ADDRESS(ES)  U.S. Army Cold Regions Research and Engineering Laboratory 72 Lyme Road Hanover, New Hampshire 03755-1290		8. PERFORMING ORGANIZATION REPORT NUMBER  CRREL Report 94-1
9. SPONSORING/MONITORING AGENCY NAME(S) AND ADDRESS(ES)  Office of the Chief of Engineers Washington, D.C. 20314-1000		10. SPONSORING/MONITORING AGENCY REPORT NUMBER

11. SUPPLEMENTARY NOTES  Additional funding provided by Technical Research Institute, Konoike Construction Co., Ltd., Konohana, Osaka, Japan	
12a. DISTRIBUTION/AVAILABILITY STATEMENT  Approved for public release; distribution is unlimited.  Available from NTIS, Springfield, Virginia 22161.	12b. DISTRIBUTION CODE

13. ABSTRACT (Maximum 200 words)  The results of an experimental study on the steady growth condition of a segregated ice layer under various applied pressures were presented in Part I. Using the data obtained, we evaluate the accuracy of the model $M_1$ , and the predicted steady growth condition is found to be in good agreement with the condition found empirically. The concept of segregation potential introduced by Konrad and Morgenstern in the early 1980s is examined based on $M_1$ . $M_1$ is found to be consistent with the empirical data that were used to support their segregation potential theory.	
---	--

14. SUBJECT TERMS  Frost heave      Frozen soils      Mathematical analysis		15. NUMBER OF PAGES 27
		16. PRICE CODE
17. SECURITY CLASSIFICATION OF REPORT  UNCLASSIFIED	18. SECURITY CLASSIFICATION OF THIS PAGE  UNCLASSIFIED	19. SECURITY CLASSIFICATION OF ABSTRACT  UNCLASSIFIED
		20. LIMITATION OF ABSTRACT  UL